molecular pharmaceutics

articles

Enhanced Cellular Respiration in Cells Exposed to Doxorubicin†

Abdul-Kader Souid,*,‡ Harvey S. Penefsky,§ Peter D. Sadowitz,‡ and Bonnie Toms‡

Department of Pediatrics, State University of New York, Upstate Medical University, 750 East Adams Street, Syracuse, New York 13210, and Public Health Research Institute, 225 Warren Street, Newark, New Jersey 07103

Received September 20, 2005

Abstract: Doxorubicin executes topoisomerase II mediated apoptosis, a process known to result in mitochondrial dysfunction, such as the leakage of cytochrome *c* and the opening of mitochondrial permeability transition pores (PTP). To further define the effects of doxorubicin on cell metabolism, we measured cellular respiration, cellular ATP, DNA fragmentation, and cytochrome *c* leakage in Jurkat (supersensitive), human leukemia-60 (HL-60, sensitive), and HL-60/MX2 (resistant) cells following exposure to 1.0 μM doxorubicin for 30 min. The measurements were made after 24 h of exposure to the drug. In Jurkat and HL-60 cells, doxorubicin treatment increased cellular mitochondrial oxygen consumption and ATP content by 2−3-fold. The increment in oxygen consumption was blocked by the pan-caspase inhibitor benzyloxycarbonyl-Val-Ala-DL-Asp-fluoromethylketone (zVAD-fmk) and by the PTP inhibitor cyclosporin A. In HL-60/MX2 cells, which are resistant because of a reduced topoisomerase II activity, doxorubicin treatment was without effect on either respiration or ATP content, suggesting that topoisomerase II was essential for induction of apoptosis and stimulation of respiration and ATP content. The conclusion that both of the latter processes were products of oxidations in the mitochondrial respiratory chain was supported by the further observation that rotenone and sodium cyanide inhibited oxygen consumption and substantially lowered ATP content in the treated and untreated cells. Thus, oxidative phosphorylation is enhanced in cells briefly incubated with doxorubicin for as long as 24 h post drug exposure despite apoptosis-associated mitochondrial insults caused by the drug.

Keywords: Doxorubicin; apoptosis; mitochondria; caspases; cell death

Introduction

Doxorubicin, an anthracycline antibiotic, is a widely used anticancer drug.[1] This agent is known to intercalate with DNA and to produce DNA breaks by stimulating topoisomerase II cleavable complex formation.[2,3] Doxorubicin induces the accumulation of the P53 tumor suppressor protein, which causes cell cycle arrest.[4] The drug also targets

* To whom correspondence should be addressed. Mailing address: Department of Pediatrics, State University of New York, Upstate Medical University, 750 East Adams Street, Syracuse, NY 13210. Tel: 315-464-5294. Fax: 315-464-7238. E-mail: souida@upstate.edu.

† The work was supported by a fund from the Paige's Butterfly Run.

‡ State University of New York.

§ Public Health Research Institute.

(1) Binaschi, M.; Bigioni, M.; Cipollone, A.; Rossi, C.; Goso, C.; Maggi, C. A.; Capranico, G.; Animati, F. Anthracyclines: Selected new developments. *Curr. Med. Chem.* **2001**, *1*, 113−130.

(2) Zunino, F.; Capranico, G. DNA topoisomerase II as the primary target of anti-tumor anthracyclines. *Anticancer Drug Des.* **1990**, *5*, 307−317.

(3) Nitiss, J. L. DNA topoisomerases in cancer chemotherapy: Using enzymes to generate selective DNA damage. *Curr. Opin. Invest. Drugs* **2002**, *3*, 1512−1516.

(4) Lorenzo, E.; Ruiz-Ruiz, C.; Quesada, A. J.; Hernandez, G.; Rodriguez, A.; Lopez-Rivas, A.; Redondo, J. M. Doxorubicin induces apoptosis and CD95 gene expression in human primary endothelial cells through a p53-dependent mechanism. *J. Biol. Chem.* **2002**, *277*, 10883−10892.

10.1021/mp050080j CCC: $33.50
Published on Web 03/01/2006

the mitochondria, impairing cellular respiration.[5−8] Other cellular targets include the sarcoplasmic reticulum, which disturbs intracellular Ca^{2+} homeostasis.[9] In the cell, the quinone moiety of doxorubicin is reduced to semiquinone radicals, generating reactive oxygen species [e.g., superoxide anion ($O_2^{\bullet}$), hydrogen peroxide (H_2O_2), and hydroxyl radical ($OH^{\bullet}$)], which can directly damage cell organelles.[5] Oxidative damage produced by the drug is partially mediated by the doxorubicin−Fe(III) complex.[10] The ultimate outcome of these events is cell death, primarily by apoptosis.[11]

Apoptosis is executed by a series of cysteine proteases, termed caspases. Caspase activation leads to mitochondrial dysfunction[12] and DNA fragmentation.[13] The mitochondrial perturbation includes the opening of the permeability transition pores (PTP). PTP are formed at contact sites between the inner and outer mitochondrial membranes. These pores are composed primarily of cyclophilin D (inhibited by cyclosporin A, CSA), the adenine nucleotide translocator (inhibited by bongkrekic acid) and the voltage-dependent anion channel.[14−20] When opened, the PTP permit passage of protons, which dissipate the mitochondrial membrane potential ($\Delta\Psi m$), leading to uncoupling of oxidative phosphorylation[18] and to passage of low molecular weight apoptogenic proteins such as cytochrome *c*. Loss of cytochrome *c* can decrease mitochondrial oxygen consumption.[21] It has been suggested that the mitochondrial perturbations are transient.[12] Blocking the PTP with CSA or bongkrekic acid restores mitochondrial functions and prevents cell death.[14,19] Because of the complex mechanisms involved in drug-induced mitochondrial dysfunction, the net effect of doxorubicin on cellular respiration remains unclear. The experiments presented here address this issue.

In the cytosol, cytochrome *c* binds to the apoptotic protease activating factor-1 (Apaf-1), which activates caspase 9.[21] The latter activates caspase 3, which executes the proteolytic and DNA fragmenting cascades.[22] DNA is initially cleaved to large fragments. Further cuts produce an oligonucleosomal ladder (≤10 000 bp), in multiples of 200 bp. Necrosis can produce similar cellular perturbations.[14]

Clinically, the maximum concentration, C_{max}, of plasma doxorubicin after 30−60 mg/m^2 iv bolus dosing is 3−10 μM, with $t_{1/2\alpha}$ of 5.0 ± 2.5 min, $t_{1/2\beta}$ 1.9 ± 0.6 h, and $t_{1/2\gamma}$ 39 ± 19 h.[23] However, cellular doxorubicin levels are usually 30−100-fold higher than those of the plasma.[23] The serious side effects of doxorubicin that limit its clinical use include cardiomyopathy, which is (at least partially) a result of drug-induced mitochondrial impairments.[5]

Endogenous low molecular weight thiols (e.g., glutathione and metallothionein) can reduce doxorubicin toxicities.[7,24] Moreover, the free thiol agent WR-1065 [*S*-2-(3-aminopropylamino)ethanethiol; $^{+}H_3N$-$(CH_2)_3$-NH_2^{+}-$(CH_2)_2$-SH]

(5) Doroshow, J. H. Effect of anthracyclines antibiotics on oxygen radical formation in rat heart. *Cancer Res.* **1983**, *43*, 460−472.
(6) Davis, K. J.; Doroshow, J. H. Redox cycling of anthracyclines by cardiac mitochondria. I. Anthracycline radical formation by NADH dehydrogenase. *J. Biol. Chem.* **1986**, *261*, 3060−3067.
(7) Wang, G.-W.; Klein, J. B.; Kang, Y. J. Metallothionein inhibits doxorubicin-induced mitochondrial cytochrome c and caspase-3 activation in cardiomyocytes. *J. Pharmacol. Exp. Ther.* **2001**, *298*, 461−468.
(8) Huigsloot, M.; Tijdens, I. B.; Mulder, G. J.; van de Water, B. Differential regulation of doxorubicin-induced mitochondrial dysfunction and apoptosis by Bcl-2 in mammary adenocarcinoma (MTLn3) cells. *J. Biol. Chem.* **2002**, *277*, 35869−35879.
(9) Zorzato, F.; Salviati, G.; Facchinetti, T.; Volpe, P. Doxorubicin induces calcium release from terminal cisternae of skeletal muscle. A study on isolated sarcoplasmic reticulum and chemically skinned fibers. *J. Biol. Chem.* **1985**, *260*, 7349−7355.
(10) Kostoryz, E. L.; Yourtee, D. M. Oxidative mutagenesis of doxorubicin-Fe(III) complex. *Mutation Res.* **2001**, *490*, 131−139.
(11) Bellarosa, D.; Ciucci, A.; Bullo, A.; Nardelli, F.; Manzini, S.; Maggi, C. A.; Goso, C. Apoptotic events in a human ovarian cancer cell line exposed to anthracyclines. *J. Pharmacol. Exp. Ther.* **2001**, *296*, 276−283.
(12) Green, D. R.; Kroemer, G. The pathophysiology of mitochondrial cell death. *Science* **2004**, *305*, 626−629.
(13) Wyllie, A. H. Glucorticoid-induced thymocyte apoptosis is associated with endogenous endonuclease activation. *Nature (London)* **1980**, *284*, 555−556.
(14) Vande Velde, C.; Cizeau, J.; Dubik, D.; Alimonti, J.; Brown, T.; Israels, S.; Hakem, R.; Greenberg, A. H. BNIP3 and genetic control of necrosis-like cell death through the mitochondrial permeability transition pore. *Mol. Cell. Biol.* **2000**, *20*, 5454−5468.
(15) Clarke, S.; McStay, G. P.; Halestrap, A. P. Sanglifehrin A acts as a potent inhibitor of the mitochondrial permeability transition and reperfusion injury of the heart by binding to cyclophilin-D at a different site from cyclosporine A. *J. Biol. Chem.* **2002**, *277*, 34793−34799.
(16) Zheng, Y.; Shi, Y.; Tian, C.; Jiang, C.; Jin, H.; Chen, J.; Almasan, A.; Tang, H.; Chen, Q. Essential role of the voltage-dependent anion channel (VDAC) in mitochondrial permeability transition pore opening and cytochrome c release induced by arsenic trioxide. *Oncogene* **2004**, *23*, 1239−1247.
(17) Di Lisa, F.; Menabo, R.; Canton, M.; Barile, M.; Bernardi, P. Opening of the mitochondrial permeability transition pore causes depletion of mitochondrial and cytosolic NAD^+ and is a cause event in the death of myocytes in postischemic reperfusion of the heart. *J. Biol. Chem.* **2001**, *276*, 2571−2575.
(18) Batandier, C.; Leverve, X.; Fontainer, E. Opening of the mitochondrial permeability transition pore induces reactive oxygen species production at the level of the respiratory chain complex I. *J. Biol. Chem.* **2004**, *279*, 17197−17204.
(19) Rajesh, K. G.; Sasaguri, S.; Ryoko, S.; Maeda, H. Mitochondrial permeability transition-pore inhibition enhances functional recovery after long-term hypothermic heart preservation. *Transplantation* **2003**, *76*, 1314−1320.
(20) Bernardi, P.; Vassanelli, S.; Veronese, P.; Colonna, R.; Szabo, I.; Zoratti, M. Modulation of the mitochondrial permeability pore. Effect of protons and divalent cations. *J. Biol. Chem.* **1992**, *267*, 2934−2939.
(21) Liu, P.; Nijhawan, D.; Budihardjo, I.; Srinvasula, S. M.; Ahmad, M.; Alnemri, E.; Wang, X. Cytochrome c and dATP-dependent formation of Apaf-1/caspase-9 complex initiates an apoptotic protease cascade. *Cell* **1997**, *91*, 479−489.
(22) Hengartner, M. O. The biochemistry of apoptosis. *Nature* **2000**, *407*, 770−776.
(23) Speth, P. A.; Linssen, P. C.; Boezeman, J. B.; Wessels, H. M.; Haanen, C. Cellular and plasma adriamycin concentrations in long-term infusion therapy of leukemia patients. *Cancer Chemother. Pharmacol.* **1987**, *20*, 305−310.

ameliorates some of the adverse effects of doxorubicin.[25] WR-1065 is the active metabolite produced by hydrolysis of the parent drug WR-2721 [*S*-2-(3-aminopropylamino)ethyl phosphorothioic acid; $^{+}H_3N$-$(CH_2)_3$-NH_2^{+}-$(CH_2)_2$-*S*-PO_3H^{-}]. The protective mechanism of WR-1065 centers on its thiol group, which reacts with free radicals and neutralizes electrophils. The C_{max} of plasma WR-1065 after 825 mg/m^2 iv infusion of WR-2721 over 15 min is 83 ± 37 μM and $t_{1/2}$ 13 ± 3 min. In the tissues, WR-1065 is converted mostly to symmetric (WR-33278) and mixed disulfides.[26]

We monitored oxygen consumption in order to quantitate the effects of doxorubicin on respiration in three malignant human cell lines.[27,28] We also measured cellular ATP, drug-induced cytochrome *c* leakage, DNA fragmentation, and doxorubicin accumulation. The results show that cyanide-sensitive respiration and an accompanying ATP synthesis are enhanced in cells incubated with doxorubicin as described for up to 24 h.

Materials and Methods

Chemicals. Solutions of doxorubicin HCl (3.45 mM) were purchased from GensiaSicor Pharmaceuticals (Irvine, CA). A 2 mM solution of zVAD-fmk was purchased from Biovision (Mountain View, CA). CSA (Sandimmune Injection) was obtained from Bedford Laboratories (Bedford, OH) as a 41.58 mM solution. WR-1065.2HCl and WR-2721 (amifostine, Ethyol) were obtained from US Bioscience (West Conshohocken, PA). A Pd(II) complex of *meso*-tetra-(4-sulfonatophenyl)-tetrabenzoporphyrin (Pd phosphor sodium salt) was purchased from Porphyrin Products (Logan, UT). Agarose (molecular biology grade) and 1 kilobase pair, kbp, DNA stepladder were purchased from Promega (Madison, WI). Dulbecco's PBS (without calcium or magnesium), fetal bovine serum (FBS), and RPMI-1640 medium (10-040) with L-glutamine (pH 7.15 ± 0.1) were purchased from Mediatech (Herndon, VA). Human (promyelocytic) leukemia (HL-60), HL-60/MX2 (CRL-2257, a mitoxantrone-resistant derivative of the HL-60 cell line), and Jurkat clone E6-1 human acute T cell leukemia (TIB-152) cell lines were purchased from American Tissue Culture Collection (Manassas, VA). Anti-cytochrome *c* (sc-13156) and horseradish peroxidase-conjugate (HRP) secondary (sc-2055) antibodies were purchased from Santa Cruz Biotechnology (Santa Cruz, CA). MagicMark Western protein standards (20−120 kDa) were purchased from Invitrogen Life Technologies (Carlsbad, CA). Complete protease inhibitor cocktail was purchased from Roche Applied Science (Indianapolis, IN). Kinetoplast DNA (kDNA) was purchased from TopoGEN (Columbus, OH). Luciferin−luciferase mixture (0.2 mg of luciferin and 22 000 units of luciferase per vial, stored at −20 °C) and ATP (2 μmol per vial, stored at −20 °C) were purchased from Chrono-Log (Havertown, PA). The remaining reagents were purchased from Sigma-Aldrich (St. Louis, MO).

Solutions. A 2 mM solution of the Pd phosphor was prepared by dissolving the powder at 2.5 mg/mL in dH_2O and stored in the refrigerator for 1 week. Ten percent perchloric acid/2 M Na methanesulfonate solution was prepared and stored as described.[26] Phosphate−citrate buffer consisted of 0.2 M Na_2HPO_4, adjusted to pH 7.8 with 0.1 M citric acid. The nonyl phenyl-polyethylene glycol (Nonidet NP-40) 0.25% (v/v) solution was made in dH_2O and stored at room temperature. The gel loading buffer contained (v/v) 0.25% bromophenol blue, 0.25% xylene cyanol FF, and 30% glycerol. The Tris-borate-EDTA buffer contained 40 mM Tris, boric acid, and 2 mM EDTA (pH 8.3). The complete protease inhibitor cocktail solution was prepared by dissolving two tablets in 0.5 mL of dH_2O (stored at −70 °C). Aqueous solutions of ATP (0.4 mM) were freshly prepared in 10 mM Tris-HEPES (pH 7.5). The final concentration was determined by absorbance at 259 using an extinction coefficient of 15 400.[29−31] A working solution of ATP (4 μM) was prepared fresh in a solution containing 0.1 M Tris-HEPES (pH 7.5), 5 mM $MgCl_2$, and 0.1% fatfree bovine serum albumin. A lyophilized powder containing luciferin (0.2 mg, mol wt 280) and luciferase (22 000 units) was freshly dissolved in 1.25 mL of PBS and protected from light. The final concentration of luciferin (570 μM) was determined from its absorbance at 327 nm, using the extinction coefficient of 18 000.[31] NaCN solutions were prepared at 0.1 M and brought to pH 7.5 with 6 N HCl.

Cells. HL-60, the resistant clone HL-60/MX2, and human T-cell lymphoma (Jurkat) cell lines were maintained in suspension cultures as described.[28] The resistance of

(24) Olson, R. D.; MacDonald, J. S.; VanBoxtel, C. J.; Boerth, R. C.; Harbison, R. D.; Slonim, A. E.; Freeman, R. W.; Oates, J. A. Regulatory role of glutathione and soluble sulfhydryl groups in the toxicity of adriamycin. *J. Pharmacol. Exp. Ther.* **1980**, *215*, 450−454.

(25) Jahnukainen, K.; Jahnukainen, T.; Salmi, T. T.; Svechnikov, K.; Eksborg, S.; Soder, O. Amifostine protects against early but not late toxic effects of doxorubicin in infant rats. *Cancer Res.* **2001**, *61*, 6423−6427.

(26) Souid, A.-K.; Fahey, R. C.; Aktas, M. K.; Sayin, O. A.; Karjoo, S.; Newton, G. L.; Sadowitz, P. D.; Dubowy, R. L.; Bernstein, M. L. Blood thiols following amifostine and mesna infusions, a Pediatric Oncology Group study. *Drug Metab. Dispos.* **2001**, *29*, 1−7.

(27) Lo, L.-W.; Koch, C. J.; Wilson, D. F. Calibration of oxygen-dependent quenching of the phosphorescence of Pd-meso-tetra (4-carboxyphenyl) porphine: A phosphor with general application for measuring oxygen concentration in biological systems. *Anal. Biochem.* **1996**, *236*, 153−160.

(28) Souid, A.-K.; Tacka, K. A.; Galvan, K. A.; Penefsky, H. S. Immediate effects of anticancer drugs on mitochondrial oxygen consumption. *Biochem. Pharmacol.* **2003**, *66*, 977−987.

(29) Balzi, E.; Chen, W.; Ulazsewski, S.; Capieaux, E.; Goffeau, A. The multidrug resistance gene PDR1 from Saccharomyces cerevisiae. *J. Biol. Chem.* **1987**, *262*, 16871−16879.

(30) Balzi, E.; Wang, M.; Leterme, S.; Van Dyk, L.; Goffeau, A. PDR5, a novel yeast multidrug resistance conferring transporter controlled by the transcription regulator PDR1. *J. Biol. Chem.* **1994**, *269*, 2206−2214.

(31) Lemasters, J. J.; Hackenbrock, C. R. Continuous measurements of adenosine triphosphate with firefly luciferase luminescence. *Methods Enzymol.* **1979**, *56*, 530−544.

HL-60/MX2 is not mediated by P-glycoprotein, but instead exhibits an altered Topo II catalytic activity and reduced levels of topoisomerase II α and β proteins.[32] Cell count and viability were determined by light microscopy, using a hemocytometer under standard trypan blue staining conditions. Mean (SD) cell volume, 170 (55) fL, was determined on the Coulter Z2 model (Beckman Coulter, Inc.).

Incubation with Drugs. Incubations were carried out in medium plus 10% fetal bovine serum at 37 °C. Unless otherwise indicated, cells were incubated with 1.0 μM doxorubicin for 30 min. The cells were then washed with medium plus 10% fetal bovine serum to remove external doxorubicin and further incubated in medium plus 10% fetal bovine serum for 24 h.

Where indicated, cells were pretreated (at 37 °C) with 2 μM zVAD-fmk[33] for 30 min. Doxorubicin (1.0 μM) was then added and the incubations continued for an additional 30 min. The cells were washed with medium plus 10% fetal bovine serum and maintained in medium plus 10% fetal bovine serum with or without zVAD-fmk (2 μM) for 24 h before respiration was measured. CSA (a PTP inhibitor) was added to the cell suspension 1 h prior to measurement of oxygen consumption. Unless otherwise indicated, rotenone (10 μM) and NaCN (1.0 mM) additions were made during the measurement of respiration.

Cellular Respiration. Oxygen concentration in the suspension was determined as a function of time using the phosphorescence of Pd(II) *meso*-tetra-(4-sulfonatophenyl)-tetrabenzoporphyrin. The phosphorescence decay of the probe was exponential, with the reciprocal of the phosphorescence decay time (τ) being linear in oxygen concentration, according to $\tau^\circ/\tau = 1 + \tau^o k_q[O_2]$. The τ is lifetime in the presence of oxygen; τ°, lifetime in the absence of oxygen; and k_q, second-order oxygen quenching rate constant. Samples were exposed to light flashes (10/s) from a pulsed light-emitting diode array with peak output at 625 nm (OTL630A-5-10-66-E, Opto Technology, Inc., Wheeling, IL). Emitted phosphorescent light was detected by a Hamamatsu photomultiplier tube (No. 928) after first passing through a wide-band interference filter centered at 800 nm. The amplified phosphorescence decay was digitized at a rate of 1 MHz by a 20 MHz A/D converter (Computer Boards, Inc.). Two hundred fifty samples were collected from each decay curve, and the data from 10 consecutive decay curves were averaged for calculating τ. The instrument was calibrated using ascorbate and ascorbate oxidase as described.[27]

Cellular respiration was measured at 25 °C in sealed vials containing 1.3×10^7 cells per condition.[28,33,34] The cells were suspended in 0.5 mL (final volume) of Pd phosphor solution [RPMI medium (containing 6.0 mM Na_2HPO_4 and 10 mM glucose) supplemented with 2 μM Pd phosphor and 3% (w/v) fatfree bovine serum albumin (pH, 7.5)]. The solution was freshly made and continuously stirred for 30 min prior to use. Cellular respiration was determined as the negative slope of the curve of $[O_2]$ vs time (zero-order rate constant, k, in μM O_2 min^{-1} per 1.3×10^7 cells). The values of k were linear with the cell counts.[33] The value of k for the Pd phosphor solution without cells was (mean ± SD) 0.28 ± 0.05 μM O_2 min^{-1}. In the presence of rotenone, the value of k for 10^7 cells incubated at 37 °C for 1 h with 50 μM rotenone was 0.36 ± 0.16 μM O_2 min^{-1}. Moreover, addition of 1.0 mM NaCN during measurement of respiration resulted in a complete inhibition of oxygen uptake. Thus, the decline in oxygen concentration during these measurements reflected mainly cellular mitochondrial oxygen consumption.

ATP Content. Acid extracts were prepared by adding 200 μL of 10% perchloric acid to pellets containing 10^6 cells. The mixture was sonicated on ice for 30 s, and the supernatant was collected by centrifugation (1000*g*) and neutralized by adding 200 μL of 2 M KOH. The sample was incubated on ice for 15 min, and precipitated $KClO_4$ was removed by centrifugation. The ATP content in the resulting supernatant was determined immediately. The luciferin−luciferase bioluminescence system was used to determine cellular ATP.[31,35] Luminescence was measured at 37 °C using a luminometer (Chrono-Log Corporation, Havertown, PA) connected to a potentiometric recorder (Allen Datagraph, Salem, NH). The reaction mixture contained, in a final volume of 0.4 mL, 0.1 M Tris-HEPES (pH 7.6), 5 mM $MgCl_2$, 0.1% fatfree bovine serum albumin, and ATP (40−120 pmol) or cellular acid extract (5−10 μL). The reaction was started by rapidly injecting 10 μL of luciferin−luciferase mixture (5 nmol of luciferin and 176 units of luciferase) from a 50 μL Hamilton syringe into 0.4 mL of rapidly stirred assay mixture. The luminometer was calibrated to give a light emission response of 1 mV for 1 pmol of ATP. The amount of light produced was proportional to the amount of ATP added (0−120 pmol, $r > 0.998$).

Mitochondria. All procedures were carried out at 4 °C. Cells were centrifuged for 5 min at 650*g*. The pellet was washed twice with 25 mL of a solution containing, at pH 8, 0.25 M sucrose, 2 mM EDTA, 1.0 mM nicotinamide, and 0.25 mM citrate. The washed pellet was suspended in 1.0 mL of the same solution (supplemented with 5 μL/mL complete protease inhibitor cocktail) and transferred to a Dounce homogenizer packed in ice. Homogenization was accomplished with 10−20 vigorous vertical passes of the pestle as described.[36] The homogenate was diluted to 20 mL with the same solution and centrifuged as above. The upper

(32) Harker, W. G.; Slade, D. L.; Drake, F. H.; Parr, R. L. Mitoxantrone resistance in HL-60 leukemia cells: Reduced nuclear topoisomerase II catalytic activity and drug-induced DNA cleavage in association with reduced expression of the topoisomerase II β isoform. *Biochemistry* **1991**, *30*, 9953−9961.

(33) Tacka, K. A.; Dabrowiak, J. C.; Goodisman, J.; Penefsky, H. S.; Souid, A.-K. Quantitative studies on cisplatin-induced cell death. *Chem. Res. Toxicol.* **2004**, *17*, 1102−1111.

(34) Tacka, K. A.; Szalda, D.; Souid, A.-K.; Goodisman, J.; Dabrowiak, J. C. Experimental and theoretical studies on the pharmacodynamics of cisplatin in Jurkat cells. *Chem. Res. Toxicol.* **2004**, *17*, 1434−1444.

(35) Karamohamed, S.; Guidotti, G. Bioluminometric method for real-time detection of ATPase activity. *BioTechniques* **2001**, *31*, 420−425.

80% of the supernatant was carefully collected and centrifuged for 10 min at 900*g*. The top upper 80% of the resulting supernatant was recentrifuged at 13 000*g* for 20 min. The pellet was gently rinsed and resuspended in 20 mL of the same solution. The final pellets (0.5−3.0 mg) were rinsed as above and suspended in mixture containing (in a total volume of 0.5 mL) 0.25 M sucrose, 3% fatfree albumin, 2 μM Pd phosphor, 10 mM $MgCl_2$, 10 mM KH_2PO_4 (pH 7.4), 10 mM NaF, 30 mM triethanolamine (pH 7.4), 30 mM KCl, 1.0 mM NAD^+, 1.0 mM nicotinamide, and 5 μL/mL complete protease inhibitor cocktail. Further additions were 10 mM pyruvate + malate and 50 μM FCCP.

Topoisomerase II Activity. Nuclear fractions were prepared using NE-PER extraction reagents according to the manufacturer's suggestions (Pierce Biotechnology, Rockford, IL). The reaction mixture contained 2.5 μg of nuclear extract, 0.25 μg of kDNA, 5 mM Tris-Cl (pH 8.0), 12 mM KCl, 1.0 mM $MgCl_2$, 50 μM ATP, 50 μM DTT, and 3 μg of bovine serum albumin (final volume 16 μL). The mixtures were incubated at 37 °C for 15 min. At the end of the incubation period, 4 μL of the gel-loading buffer were added. The samples were loaded on 1.0% agarose gel and electrophoresed at 120 V in Tris-borate-EDTA buffer for 1 h. The gel was then processed and analyzed as described below.

Cellular Doxorubicin Accumulation. Cells, in medium plus 10% bovine serum, were incubated with 1.0 μM doxorubicin for varying lengths of time. The cells were then collected by centrifugation (1000*g* for 1.0 min) and rapidly washed with PBS (washing time, 2 min). The cell pellets were suspended in 300 μL of 10% perchloric acid, 2 M Na methanesulfonate. The mixtures were vigorously mixed and sonicated on ice for 2.0 min. The acid-soluble supernatants were analyzed for doxorubicin on a Beckman HPLC system. The solvent was 60% of 50 mM NaH_2PO_4 (pH 3.5) and 40% of acetonitrile. The column (4.6 × 250 mm Beckman ultrasphere IP) was operated isocratically at 0.5 mL/min. Standards (10 μM doxorubicin in H_2O or 10% perchloric acid plus 2 M Na methanesulfonate) were included with each analytical run. Doxorubicin peaks were detected by fluorescence (480 nm excitation and 560 nm emission) as described.[37] The standard curves were linear ($r > 0.999$) over 50−600 pmol. The minimum quantifiable level with a signal-to-noise ratio >3:1 was 10 pmol. Peak identification was confirmed by retention time in comparison with the standards. Quantification was based on peak area against the standards. Cellular doxorubicin concentrations (expressed in micromoles/liter) were calculated as picomoles of doxorubicin (determined on HPLC) per total cell volume (cell count × mean cell volume).

DNA Fragmentation. DNA fragments were extracted essentially as described.[33,34,38] Briefly, cells (3×10^6 cells/condition) were washed with PBS and suspended in 1.0 mL of ice-cold PBS. The cells were fixed in 8.0 mL of ice-cold 70% ethanol. The suspension was incubated at −20 °C for 24 h and centrifuged (1000*g* for 5 min at 4 °C). The supernatant was discarded, and the ethanol was allowed to evaporate. The pellet was suspended in 50 μL of phosphate−citrate buffer and incubated at 20 °C for 90 min. The suspension was centrifuged (as above). The supernatant was lyophilized in the Speed Vac. The lyophilized pellet was suspended in 20 μL of a solution containing 1.55 mg of Nonidet NP-40, 60 mg of SDS, 60 μg of ribonuclease A, and 60 μg of ribonuclease T_1. After overnight incubation at 37 °C, 6 μL of proteinase k (0.12 mg) was added and the mixture was incubated overnight. Twenty-four microliters of the gel-loading buffer was added. Twenty-two microliters (corresponding to 1.3×10^6 cells) was loaded on 4 mm thick, 1.0% agarose gels, and electrophoresed at 25 V and 11 mA for 15 h in TBE buffer. Each extract was loaded on two separated gels. The gels were stained in 300 mL of 0.5 μg/mL ethidium bromide for 30 min in the dark. After destaining for 15 min in dH_2O, the gels were stored at 4 °C in 300 mL of TBE. The images were captured using a Gel Doc digital camera system with Quantity One software (Bio-Rad). The digital image was analyzed using Sigma Scan software (version 2.0, SPSS Inc.). Individual lanes were scanned with a broad line (17 pixels wide) from the loading well to the end of the streaks. The net fluorescence intensity was calculated as the total intensity minus the background.

Protein Immunoblot Analysis. Cytosolic fractions were prepared using NE-PER extraction reagents according to the manufacturer's suggestions (Pierce Biotechnology, Rockford, IL). Five microliters of complete protease inhibitor cocktail solution was added to each milliliter of the extraction solutions. The protein content was measured by the Quick Start Bradford protein assay kit, using bovine serum albumin as standard (Bio-Rad Laboratories, Hercules, CA). Samples were diluted with equal volumes of Laemmli loading buffer (62.5 mM Tris-Cl, pH 6.8, 2% SDS, 25% glycerol, 0.01% bromophenol blue, and 715 mM β-mercaptoethanol). Protein samples, about 10 μg per condition, were loaded on 10−20% gradient SDS−PAGE and electrophoresed at 120 V for 90 min. The running buffer consisted of 25 mM Tris-base, 250 mM glycine, and 1% (wt/vol) SDS. The proteins were transferred to polyvinylidene difluoride membranes (at 290 mA for 60 min in 50 mM Tris-base and 400 mM glycine). The blots were blocked with 5% (w/v) nonfat dry milk in PBS plus 0.1% (vol/vol) Tween-20 for 1.0 h. The blots were then washed (10 min × 3) with PBS-Tween-20, and probed for cytochrome *c* (2 μg/mL in 1% nonfat dry milk in PBS-Tween-20) at 4 °C overnight. Blots were washed (10 min ×

(36) Wu, R.; Sauer, L. Preparation and assay of phosphorylating mitochondria from ascites tumor cells. *Methods Enzymol.* **1967**, *10*, 105−110.

(37) Fogli, S.; Danesi, R.; Innocenti, F.; Di Paolo, A.; Bocci, G.; Barbara, C.; Del Tacca, M. An improved HPLC method for therapeutic drug monitoring of daunorubicin, idarubicin, doxorubicin, epirubicin, and their 13-dihydro metabolites in human plasma. *Ther. Drug Monit.* **1999**, *21*, 367−376.

(38) Gong, J.; Traganos, F.; Darzynkiewicz, Z. A selective procedure for DNA extraction from apoptotic cells applicable for gel electrophoresis and flow cytometry. *Anal. Biochem.* **1994**, *218*, 314−319.

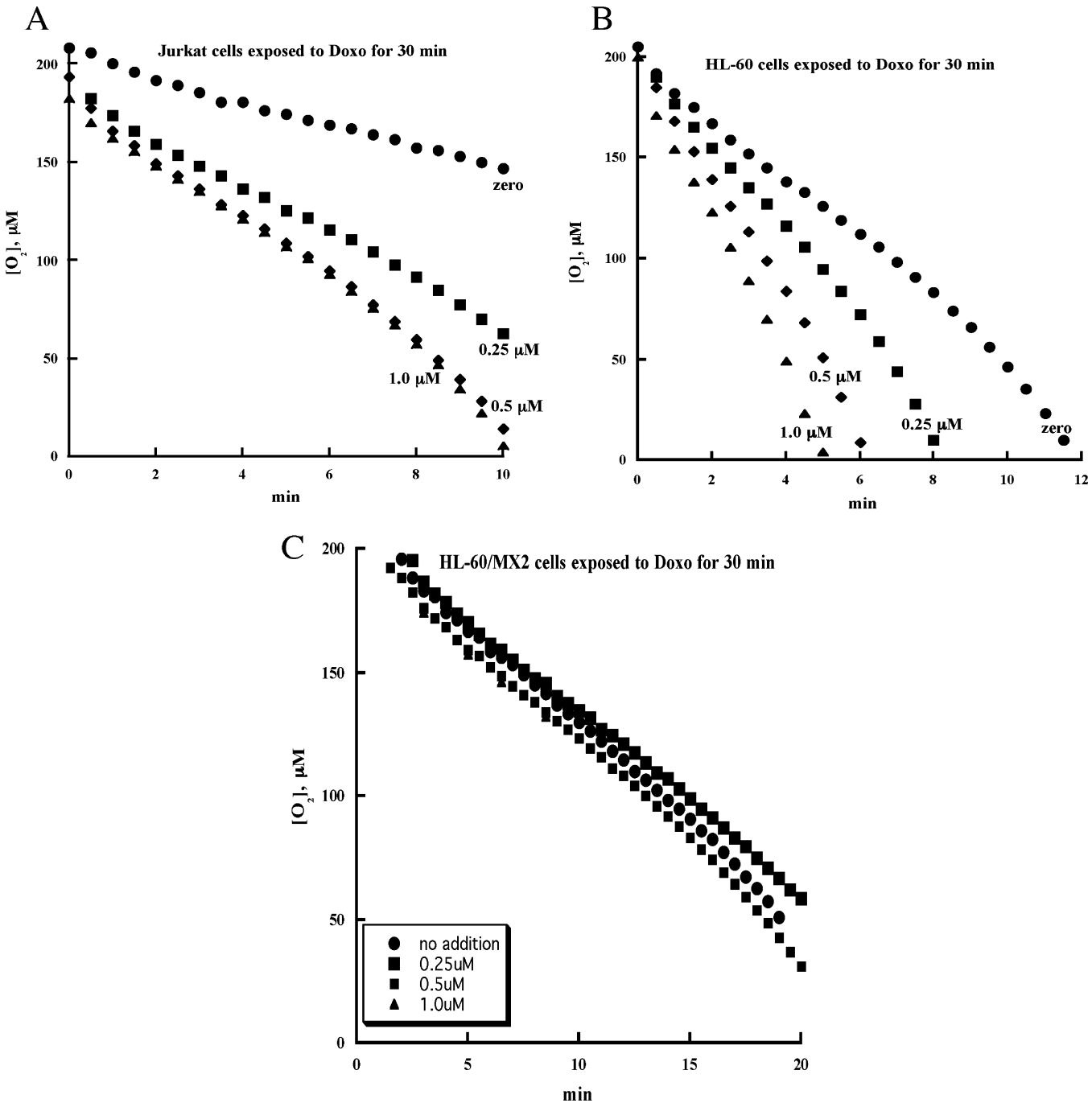

Figure 1. Effects of doxorubicin on cellular respiration. Representative experiments are shown. Jurkat (A), HL-60 (B), and HL-60/MX2 (C) cells were incubated for 30 min with 0 (circles), 0.25 (squares), 0.5 (diamonds), and 1.0 (triangles) μM doxorubicin. At h 24, the cells were suspended in Pd phosphor solution and oxygen consumption was measured as described in Materials and Methods. The values of *k* are summarized in Table 1.

3) with PBS-T, and incubated with secondary antibodies (1 μg/mL in 1% nonfat dry milk in PBS-Tween-20). The blots were washed with PBS-Tween-20 (10 min × 3) and PBS (10 min × 1). Cytochrome *c* was visualized by an enhanced chemiluminesence, using ECL detection kit (Amersham Pharmacia Biotech, U.K.).

Statistical Analysis. The significance between values under different experimental conditions was determined by paired Student's *t*-test analyses. A value of $p < 0.05$ was considered significant.

Results

Effects of Doxorubicin on Cellular Respiration and Modulations by zVAD-fmk, CSA, and WR-1065. Table 1 and Figure 1 show the effects of doxorubicin on cellular mitochondrial oxygen consumption. The cells were exposed

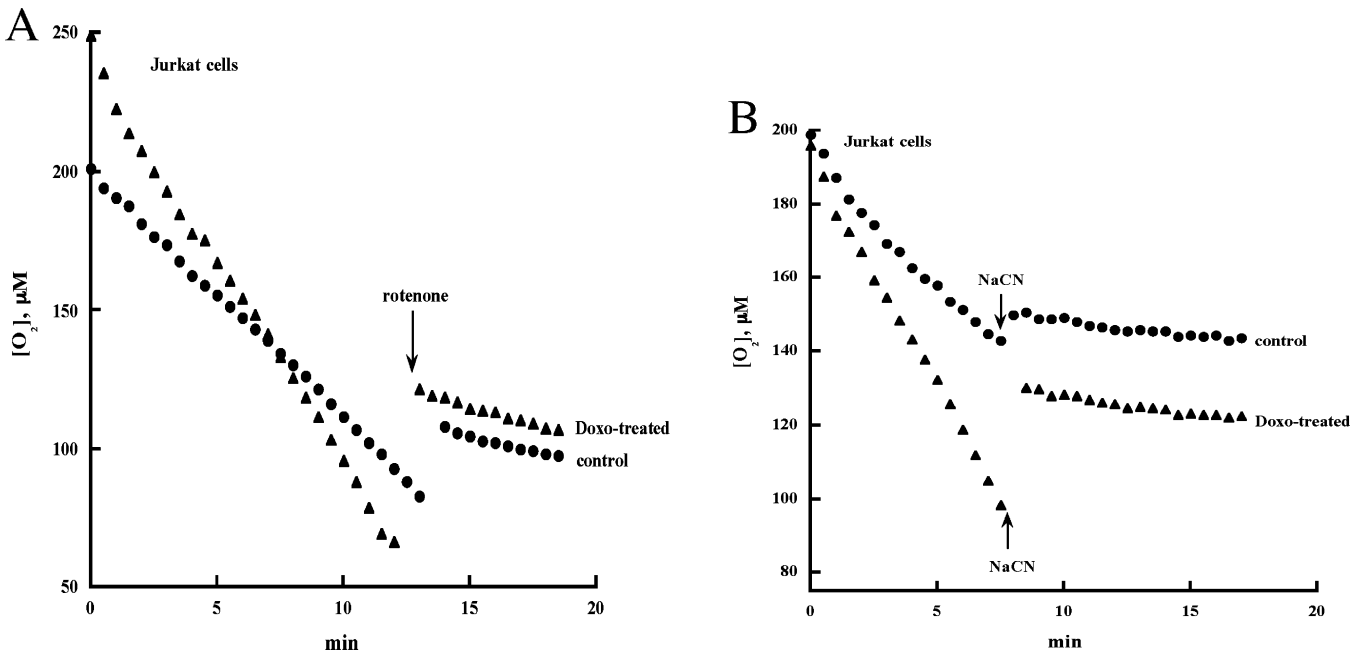

Figure 2. Rotenone- and NaCN-induced inhibition of cellular respiration in treated and untreated cells. Jurkat cells were incubated with (triangles) and without (circles) 1 μM doxorubicin for 30 min. At h 24, the cells were suspended in Pd phosphor solution and oxygen consumption was measured as described in Materials and Methods. Where indicated, 5 μM rotenone and 1 mM NaCN were added.

Table 1. Effect of Doxorubicin on Cellular Respiration[a]

	values of k (μM O_2 min^{-1} per 1.3×10^7 cells)		
[doxo] (μM)	Jurkat	HL-60	HL-60/MX2
0	4.6 ± 0.8 (3)	13.0 ± 2.7 (4)	8.0 ± 0.3 (3)
0.25	12.2 ± 0.1 (3)[b]	18.4 ± 4.0 (4)[c]	8.0 ± 0.3 (3)
0.5	16.2 ± 0.3 (3)[b]	26.4 ± 6.9 (4)[c]	8.0 ± 0.3 (3)
1.0	13.3 ± 4.3 (3)[c]	28.1 ± 7.3 (4)[c]	8.0 ± 0.3 (3)

[a] Cells were exposed to doxorubicin for 30 min. At h 24, the cells were suspended in Pd phosphor solution and oxygen consumption was measured as described in Materials and Methods. The values of k [mean $\pm$ SD (n)] were determined as the negative slopes of the curves of [O_2] versus time ($r > 0.99$), Figure 1. For all cell types, the values of k decreased by more than 80% in the presence of 10 μM rotenone. [b] The p values between the untreated and treated cells are <0.005. [c] The p values between the untreated and treated cells are <0.05.

Table 2. Modulation of Doxorubicin Effects on Cellular Respiration and DNA Fragmentation by WR-1065[a]

[doxo]	WR-1065	k	fragment intensities
0	0	4.6	6.0 ± 0.9
0	150 μM for 24 h	4.4	4.0 ± 0.1
1.0 μM for 15 min	0	11.1	25.3 ± 2.2[b]
1.0 μM for 15 min	150 μM for 24 h	7.9	18.9 ± 0[b]

[a] Jurkat cells were incubated with and without doxorubicin (1.0 μM for 15 min) in the presence and absence of WR-1065 (150 μM for 24 h). Cellular respiration (k, in μM O_2 min^{-1} per 1.3×10^7 viable cells; $r > 0.99$) and DNA fragmentation (mean $\pm$ SD of 3 separate experiments, arbitrary units/10^3) were determined 24 h after doxorubicin exposure. [b] The p values between the two conditions are <0.05.

to 0.25−1.0 μM doxorubicin for 30 min, external doxorubicin was removed by washing, and cellular respiration was measured after 24 h of further incubation in drug-free medium. In both cell types, doxorubicin treatment increased the values of k (the negative slopes of the curves) by 2−3-fold (Table 1 and Figure 1A,B). In contrast, in HL-60/MX2 cells, the value of k was not affected by doxorubicin, Table 1 and Figure 1C.

In the presence of rotenone, the rate of cellular mitochondrial oxygen consumption decreased 81% in untreated cells and 89% in doxorubicin-treated cells (Figure 2A). Cellular mitochondrial oxygen consumption was fully inhibited by NaCN (Figure 2B). Very similar results were observed for HL-60 cells (data not shown).

The effects of zVAD-fmk on doxorubicin-induced enhancements of cellular mitochondrial oxygen consumption are shown in Figure 3A−C. For Jurkat cells (Figure 3A), the value of k (μM O_2 min^{-1} per 1.3×10^7 cells) for the cells incubated with no addition was 4.3, for the cells incubated with 24 h zVAD-fmk 4.9 (not shown), for the cells incubated with doxorubicin alone 16.2, for the cells incubated with doxorubicin plus 1 h zVAD-fmk 6.7, and for the cells incubated with doxorubicin plus 24 h zVAD-fmk 3.9. For HL-60 cells (Figure 3B), the value of k for the cells incubated with no addition was 14.6, for the cells incubated with doxorubicin alone 33.9, for the cells incubated with doxorubicin plus 1 h zVAD-fmk 16.8, and for the cells incubated with doxorubicin plus 24 h zVAD-fmk 13.0. Thus, for both cell lines, doxorubicin increased the value of k more than 2-fold and zVAD-fmk prevented these enhancements. In contrast, for HL-60/MX2 cells (Figure 3C), the value of k was unaffected by doxorubicin alone or doxorubicin plus zVAD-fmk. Again, zVAD-fmk alone had no effect on cellular respiration.

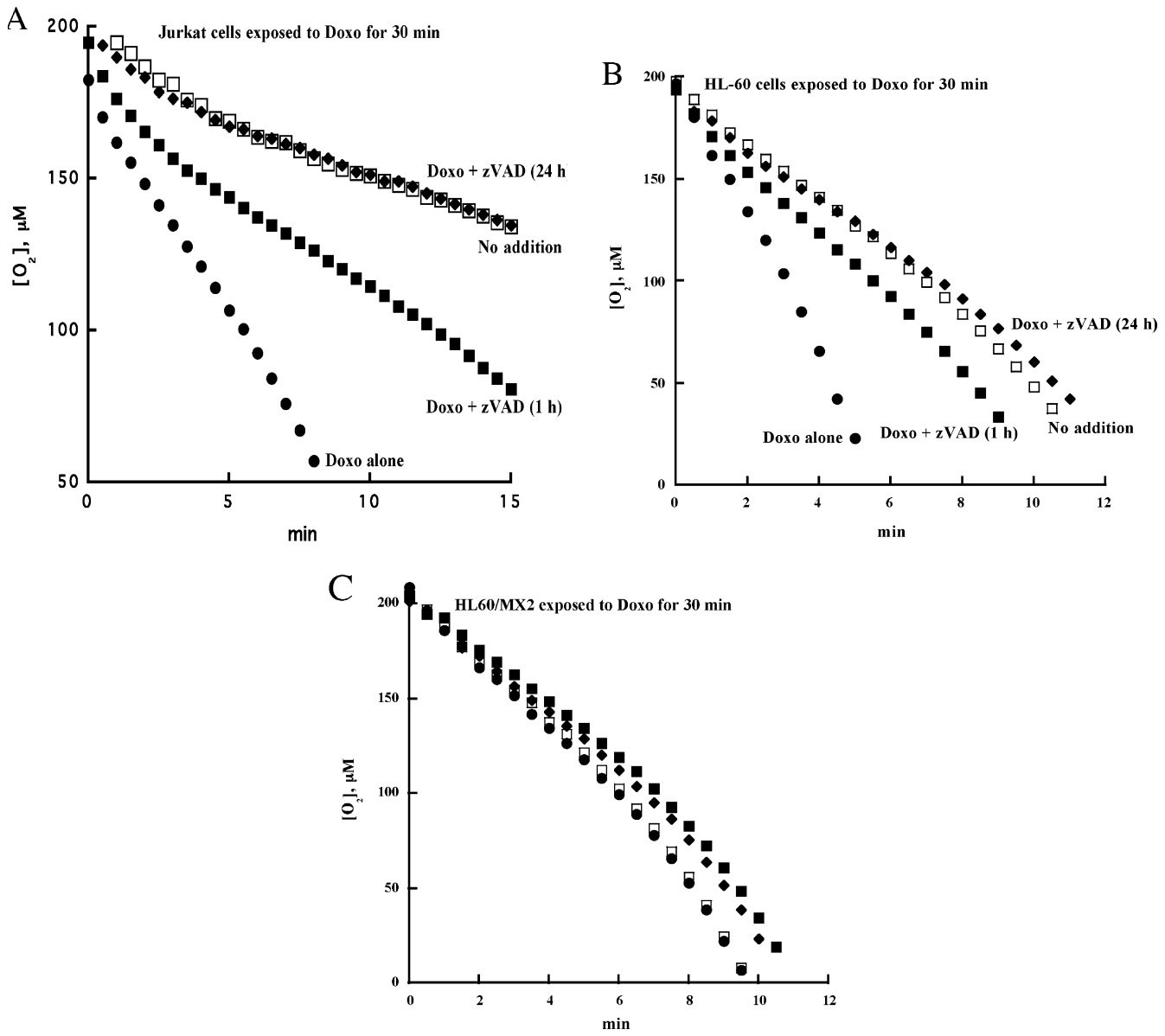

Figure 3. Modulation of doxorubicin effect on cellular respiration by zVAD-fmk. Jurkat (A), HL-60 (B), and HL-60/MX2 (C) cells were preincubated for 30 min with and without 2.0 μM zVAD-fmk. Doxorubicin (1.0 μM) was added and the incubations continued for 30 min. The cells were then maintained in medium with and without zVAD-fmk for 24 h. At h 24, the cells were suspended in Pd phosphor solution and oxygen consumption was measured as described in Materials and Methods. The data are representative of 3 separate experiments for each cell line.

The effects of CSA, an inhibitor of the PTP, on doxorubicin-induced enhancements of cellular mitochondrial oxygen consumption are shown in Figure 4. CSA was added to the cell suspensions 1 h prior to oxygen measurements. For Jurkat cells (Figure 4A), the value of k (μM O_2 min^{-1} per 1.3×10^7 cells) for the cells exposed to no drugs was 11.6, for the cells exposed to 100 μM CSA alone 10.5, for the cells exposed to doxorubicin alone 26.7, for the cells exposed to doxorubicin plus 50 μM CSA 14.9 (data not shown), and for the cells exposed to doxorubicin plus 100 μM CSA 10.5. For HL-60 cells (Figure 4B), the value of k (μM O_2 min^{-1} per 1.3×10^7 cells) for the cells exposed to no drugs was 15.2, for the cells exposed to CSA alone 12.6, for the cells exposed to doxorubicin alone 29.8, and for the cells exposed to doxorubicin plus 10 μM CSA 16.3 (the latter value was the same for the cells exposed to doxorubicin plus 20 or 30 μM CSA, data not shown). Thus, HL-60 cells were more sensitive to CSA than Jurkat cells. Nevertheless, for both cell types, doxorubicin treatment increased the rate of respiration and CSA prevented the increase. These findings suggested that the PTP participated in or were responsible for the doxorubicin-induced enhancements of cellular respiration.

The ability of WR-1065 to modulate the effect of doxorubicin on Jurkat cell respiration is shown in Table 2. Doxorubicin alone increased the value of k by 2.4-fold and doxorubicin plus WR-1065 by 1.7-fold, a protection of about

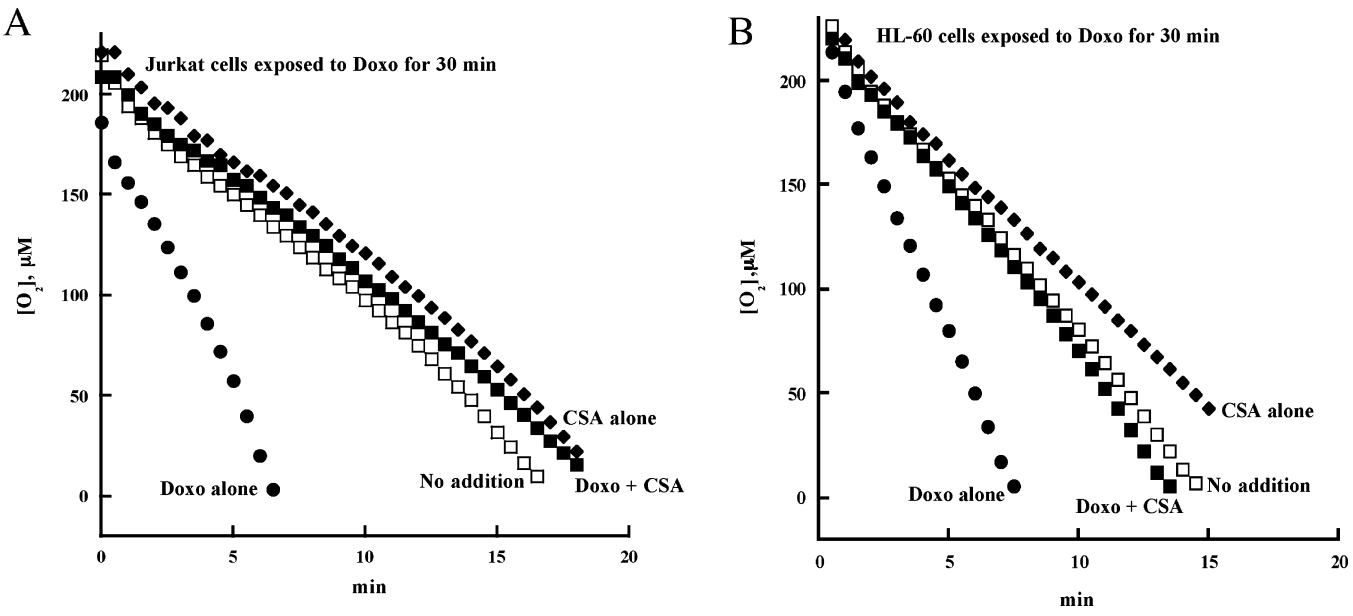

Figure 4. Modulation of doxorubicin effect on cellular respiration by CSA. Jurkat (A) and HL-60 (B) cells were incubated for 30 min with 1.0 μM doxorubicin. The cells were maintained in drug-free medium for 24 h. At h 24, CSA (100 μM for Jurkat cells and 10 μM for HL-60 cells) was added to the cell cultures for 1 h. The cells were then suspended in Pd phosphor solution and oxygen consumption was measured as described in Materials and Methods.

30%. A similar partial protection was observed in HL-60 cells (data not shown).

Cellular ATP Content. Cells were exposed to 1.0 μM doxorubicin for 30 min. Doxorubicin in the medium was then removed by washing, and total cell ATP was measured after an additional 24 h incubation in drug-free medium. The ATP content of untreated Jurkat cells was 5.8 $\pm$ 0.5 nmol/10^6 cells and doxorubicin-treated cells 20 $\pm$ 0 nmol/10^6 cells. The ATP content of untreated HL-60 cells was 3.4 $\pm$ 0.3 nmol/10^6 cells and doxorubicin-treated cells 7.4 $\pm$ 0.3 nmol/10^6 cells. The content of ATP in untreated HL-60/MX2 cells was 3.6 $\pm$ 0.5 nmol/10^6 cells and in doxorubicin-treated cells 3.2 $\pm$ 0.5 nmol/10^6 cells. In the presence of rotenone (10 μM at 37 °C for 60 min), the content of ATP in treated and untreated cells decreased by more than 80%.

Effect of Doxorubicin on Cell Replication. The proliferation of Jurkat, HL-60, and HL-60/MX2 cells, measured as the cell count, was determined 24 h (Figure 5A) and 48 h (Figure 5B) after doxorubicin exposure (0.25−1.0 μM for 30 min). Doxorubicin treatment (1.0 μM for 30 min) inhibited the growth of Jurkat and HL-60 cells. In contrast, the same treatment had no effect on the growth of HL-60/MX2 cells.

Topoisomerase II Activity. Topoisomerase II activities in nuclear extracts (prepared 24 h after doxorubicin exposure) of cells treated and untreated with doxorubicin are shown in Figure 6. Significant topoisomerase II activity (reflected by the generation of decatenated forms of kDNA) was present in the nuclear extracts of untreated Jurkat and HL-60 cells. Moreover, in both cell lines, doxorubicin treatment increased topoisomerase II activity, especially in Jurkat cells. In contrast, decatenated kDNA was not present in HL-60/MX2 cells, confirming the lack of topoisomerase II activity.

Cellular Doxorubicin Accumulation. A representative chromatograph for HL-60 cells incubated with no addition is shown in Figure 7A, and for HL-60 cells incubated with 1.0 μM doxorubicin for 15 min in Figure 7B. Representative experiments (3−7 experiments for each cell line) for cellular doxorubicin accumulation are shown in Figure 7C. These cells also were incubated for 15 min with 1.0 μM. Doxorubicin uptake during the first 60 min of exposure was 2.6 μM/min in Jurkat cells (r > 0.99), 1.2 μM/min in HL-60 cells (r > 0.98), and 1.8 μM/min in HL-60/MX2 cells (r > 0.99), Figure 7C. Because of expected drug leakage during the washing procedure, these values should be considered as minimum estimations. Nevertheless, they show that the drug uptake by Jurkat cells at 30 min was more than twice as great as the uptake by HL-60 cells.

Doxorubicin-Induced DNA Fragmentation and Modulations by zVAD-fmk and WR-1065. DNA fragmentation in Jurkat cells treated with doxorubicin (1.0 μM for 30 min) or doxorubicin plus zVAD-fmk (2.0 μM for 1 or 24 h) was measured 24 h after exposure to doxorubicin (Figure 8). The fragment intensity (arbitrary units/10^3) for cells incubated with no addition was 2.7 (lane 1), for cells incubated with 24 h zVAD-fmk 3.1 (lane 3), for cells incubated with doxorubicin alone 26.0 (lane 5), for cells incubated with doxorubicin plus 1 h zVAD-fmk 18.9 (lane 7), and for cells incubated with doxorubicin plus 24 h zVAD-fmk 17.9 (lane 9). Thus, doxorubicin (1.0 μM for 30 min) produced DNA fragmentation in Jurkat cells, and zVAD-fmk reduced the fragment intensity by about 30%. In contrast, doxorubicin treatment produced much less DNA fragmentation in HL-60 (Figure 9A, circles) and HL-60/MX2 cells (data not shown).

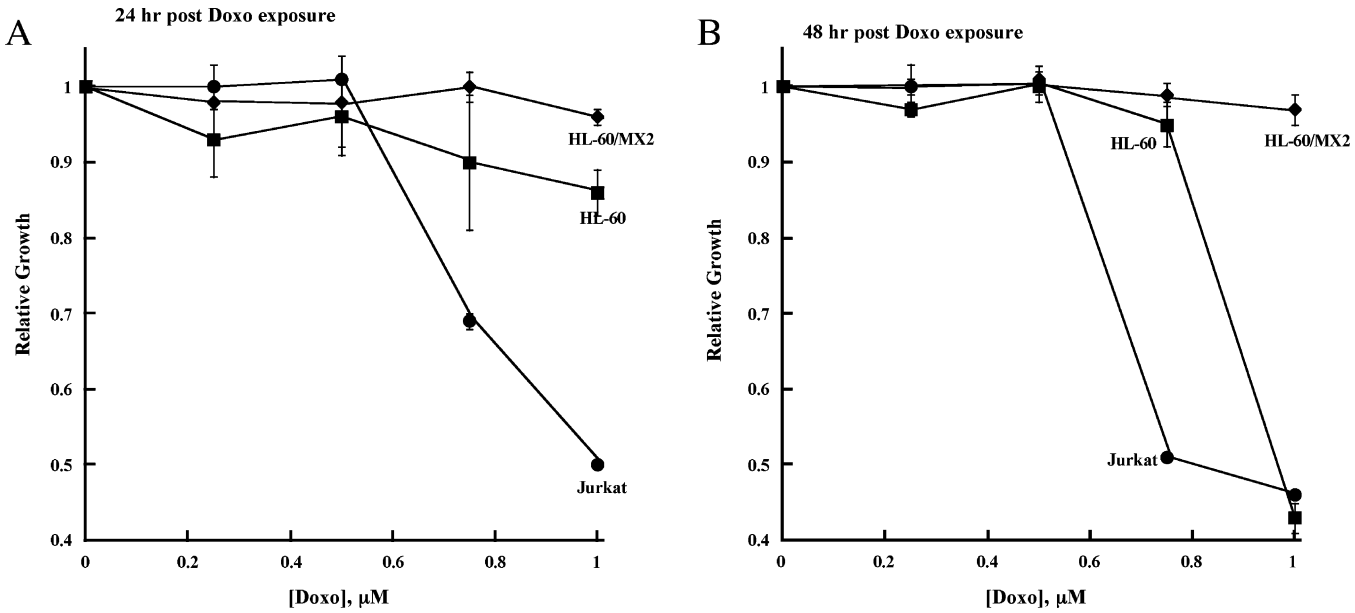

Figure 5. Effects of doxorubicin on cell replication. Jurkat (circles), HL-60 (squares), and HL-60/MX2 (diamonds) cells were incubated with indicated concentrations of doxorubicin for 30 min. The cells were then maintained in doxorubicin-free medium for 24 h (A) or 48 h (B). Relative growth was determined as the cell count reached by the treated cells divided by the cell count reached by the untreated cells at 24 and 48 h for each cell line. The results are mean ± SD of 3 independent experiments.

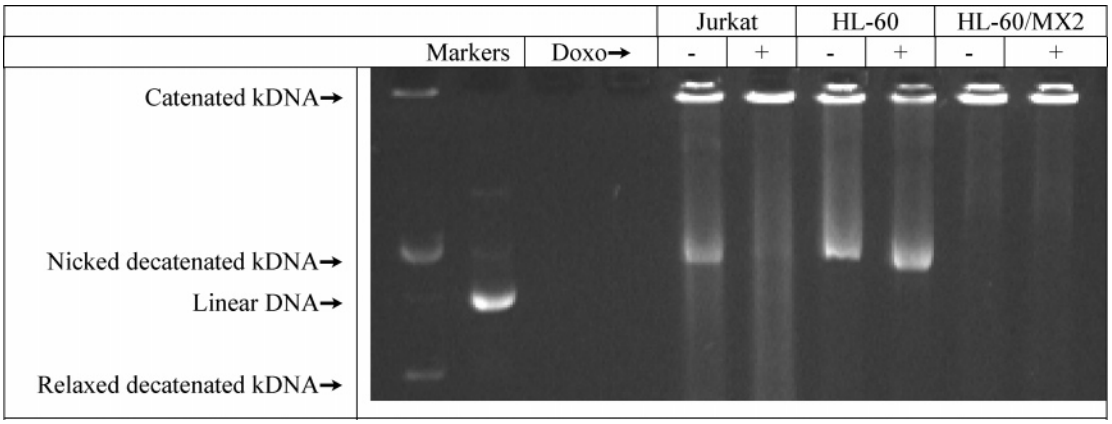

Figure 6. Decatenation of kDNA by nuclear extracts of Jurkat, HL-60, and HL-60/MX2 cells. The cells were incubated at 37 °C with and without 1.0 μM doxorubicin for 30 min. At the end of the incubation period, the cells were maintained in drug-free medium for 24 h. Nuclear extracts were then prepared as described in Materials and Methods. Decatenated kDNA (the two forms that entered the gel) was produced by topoisomerase II activities in the nuclear extracts of Jurkat and HL-60 cells. In contrast, decatenated kDNA was not present in HL-60/MX2 cells. Data are representative of 3 separate experiments using the same nuclear extracts.

The protective effects of WR-1065 (150 μM for 24 h) on doxorubicin-induced DNA fragmentation are shown in Table 2 and Figure 9. In Jurkat cells, WR-1065 decreased production of doxorubicin-induced DNA fragmentation by about 25% (Table 2). Similar protections were observed for the 30−90 min incubations with doxorubicin. Unexpectedly, WR-1065 increased doxorubicin-induced DNA fragmentation in HL-60 cells (Figure 9A).

To determine if the free thiol group of WR-1065 was responsible for the protection of DNA in Jurkat cells, the same experiments were repeated using the parent compound WR-2721. In Jurkat cells, the fragment intensity (arbitrary units/10^3) without any addition was (mean ± SD, $n = 3$) 6.9 ± 0.9, with WR-2721 alone (150 μM for 24 h) 5.1 ± 0.5, with doxorubicin alone (1.0 μM for 30 min) 25.3 ± 2.2, and with doxorubicin plus WR-2721 32.8 ± 2.5.

Doxorubicin-Induced Cytochrome *c* Release. Doxorubicin-induced cytochrome *c* leakage (measured 24 h after drug exposure) was investigated in Jurkat and HL-60 cells. Cytochrome *c* was present in the cytosolic extracts of untreated Jurkat and HL-60 cells (Figure 10, lanes 1 and 6, respectively), which could represent a background leakage of cytochrome *c* or a mitochondrial contamination of the cytosolic extracts. Nevertheless, the amount of cytochrome *c* appearing in the cytosol significantly increased with increasing exposure time to doxorubicin (Figure 10).

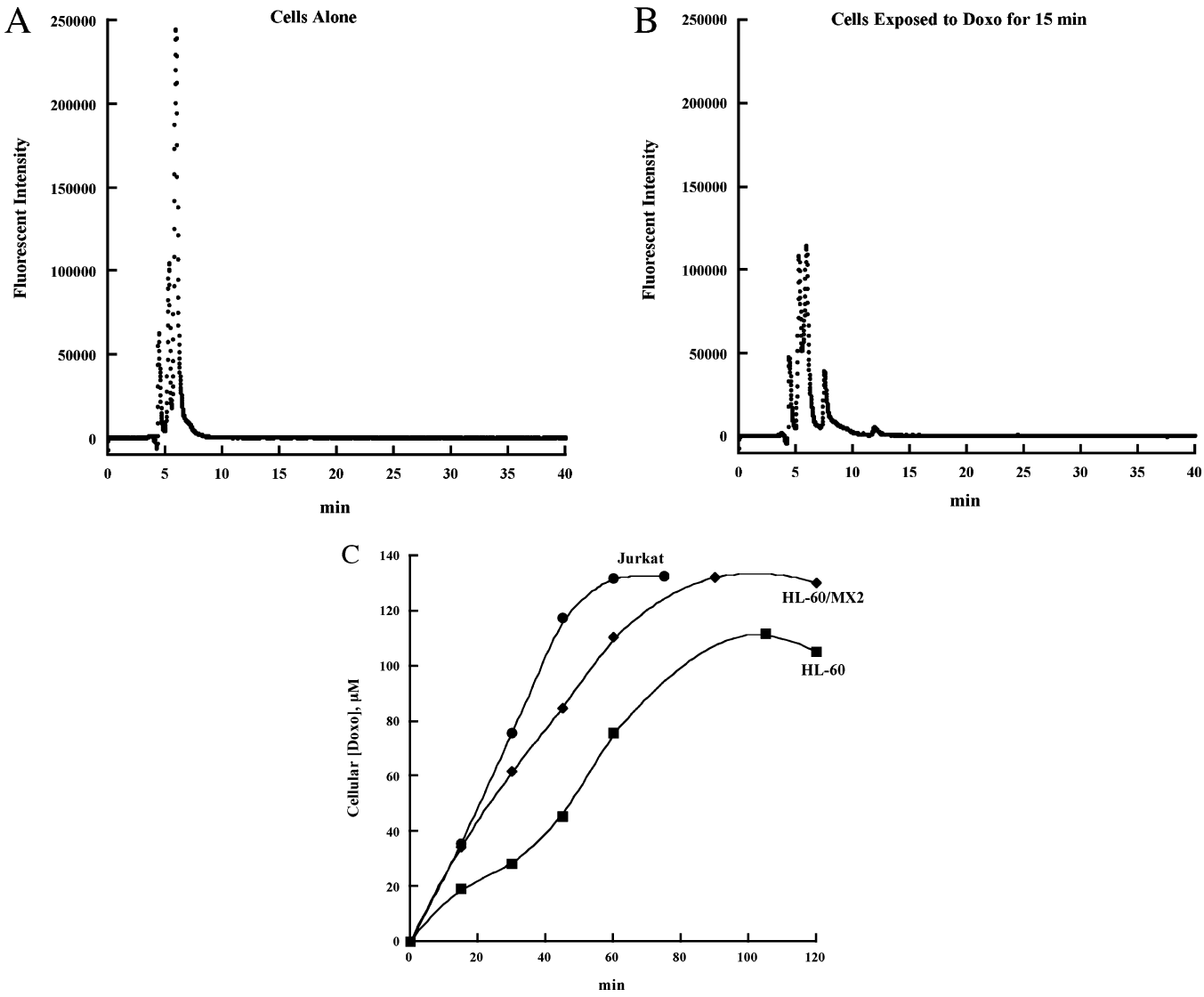

Figure 7. Representative HPLC chromatographs for untreated HL-60 cells (A) and HL-60 cells exposed to 1.0 μM doxorubicin for 15 min (B). The doxorubicin peak appeared with a retention time (t_R) of 7.5 min. The peak with t_R 12 min is a doxorubicin metabolite. Both peaks were added for doxorubicin quantitation. Cells ($0.1-1.5 \times 10^8$ cells/condition) were incubated with 1.0 μM doxorubicin for indicated periods of time. The cells were then rapidly washed with PBS, and the acid-soluble supernatants were separated on HPLC. Doxorubicin peaks were detected by fluorescence. The initial rate (C) for doxorubicin accumulation in Jurkat cells was 2.6 μM/min (circles, $r > 0.99$), in HL-60 cells 1.2 μM/min (squares, $r > 0.98$), and in HL-60/MX2 1.8 μM/min (diamonds, $r > 0.99$). The data are representative of 3−7 separate determinations for each cell type.

Oxygen Consumption by Isolated Mitochondria from Treated and Untreated Cells. Jurkat cells were exposed to 1.0 μM doxorubicin for 30 min. At the end of the incubation period, the cells were washed and incubated in drug-free medium for 24 h. Mitochondria were then isolated and oxygen consumption was determined immediately. FCCP enhanced malate + pyruvate driven respiration in untreated and treated Jurkat cells by about 3-fold (Figure 11).

Discussion

Despite the fact that anthracyclines target the mitochondria,[5−8] to our knowledge the effect of this class of agents on oxidative phosphorylation within tumor cells has not previously been quantitated. Incubation of beef-heart submitochondrial particles with ≥25 μM doxorubicin for 60 min produced no noticeable effects on oxygen consumption.[28] Thus, the effects of doxorubicin on cellular respiration in these experiments is likely indirect, mediated by induction of apoptosis or necrosis; both processes are known to produce mitochondrial injuries (e.g., leakage of cytochrome *c* and opening of the mitochondrial PTP). Addition of rotenone and cyanide in these experiments inhibited respiration, Figure 2A,B, thus establishing that the observed consumption of O_2 occurred in the respiratory chain. We also utilized zVAD-fmk (pan-caspase family inhibitor)[39] and CSA (PTP inhibitor) to investigate the role of apoptotic (necrotic) signals in modulating cellular respiration by doxorubicin. Resistant (HL-60/MX2) and sensitive (HL-60 and Jurkat) cell lines

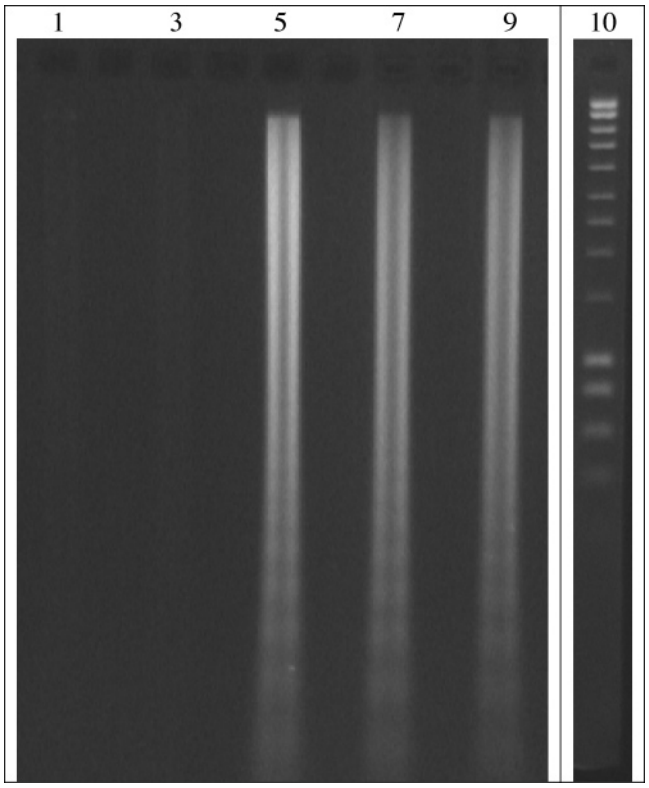

Figure 8. Doxorubicin-induced DNA fragmentation in the presence and absence of zVAD-fmk. Jurkat cells were preincubated for 30 min with and without 2.0 μM zVAD-fmk. Doxorubicin (1.0 μM) was added and the incubations continued for 30 min. The cells were then maintained in medium with and without 2.0 μM zVAD-fmk for 24 h. DNA fragmentation was measured 24 h post doxorubicin exposure. Lane 1: Cells incubated with no addition. Lane 3: Cells incubated with zVAD-fmk for 24 h. Lane 5: Cells incubated with doxorubicin alone. Lane 7: Cells incubated with doxorubicin plus 1 h zVAD-fmk. Lane 9: Cells incubated with doxorubicin plus 24 h zVAD-fmk. Lane 10: 1−10 kbp DNA stepladder.

were used to explore expected variations in the effect of doxorubicin on cellular respiration. The cells were incubated with clinically relevant concentrations of doxorubicin (0.25−1.0 μM) for 30 min. To uncover the impact of doxorubicin treatment, cellular mitochondrial oxygen consumption (Table 1), cellular ATP, DNA fragmentation (Figures 8 and 9), and cytochrome *c* leakage (Figure 10) were determined 24 h after drug exposure.[8] The 24 h exposure to zVAD-fmk (when added) is necessary since doxorubicin was retained in the cells for over 24 h (unpublished observation). It should be noted that doxorubicin treatment at concentration >1.0 μM or at incubation periods with the drug >30 min will not be readily comparable to the experiments described here.

To investigate cellular doxorubicin pharmacology, acid/salt extracts of the cells were fractionated on HPLC and their doxorubicin content was quantitated by fluorescence analysis (Figure 7). This method measures free (unbound) drug within the cell.[26] Near linear drug accumulations were observed over 45−60 min in the three cell lines studied. The initial uptake in Jurkat cells was 2.6 μM/min ($r > 0.99$), in HL-60 cells 1.2 μM/min ($r > 0.98$), and in HL-60/MX2 cells 1.8 μM/min ($r > 0.99$), Figure 7C. At 60 min, cellular doxorubicin content in Jurkat cells averaged 22.4 pmol/10^6 cells (133 μM, $n = 3$), in HL-60 cells 15.3 pmol/10^6 cells (90 μM, $n = 4$), and in HL-60/MX2 cells 19.9 pmol/10^6 cells (117 μM, $n = 3$). Thus, the concentration of doxorubicin in these cells was enhanced 90−133-fold over that in the medium.

Doxorubicin pharmacology has been studied in several cell lines. The uptake of doxorubicin by HeLa cells incubated with 0.86 μM concentrations of the drug was linear ($r > 0.99$) over 60 min; cellular doxorubicin content at min 60 was 100 pmol/10^6 cells.[40] Pancreatic adenocarcinoma cells, when incubated with 1.7 μM doxorubicin for 60 min, exhibited a drug content of 130−195 pmol/10^6 cells.[41] In both studies, total fluorescence intensities of the ethanol/acid cellular extracts (without HPLC separation) were measured. Radiolabeled doxorubicin uptake by ovarian carcinoma cells, incubated with the drug at a concentration of 0.5 μM, was linear ($r > 0.99$) for 120 min.[42] Cellular doxorubicin content at min 60 was 4 pmol/10^6 cells. Near linear doxorubicin uptake also was reported in other cell lines over 120 min.[43,44]

An essential role for topoisomerase II in doxorubicin-induced apoptosis and in the enhancement of cellular mitochondrial oxygen consumption also emerged from these studies. A brief exposure of Jurkat and HL-60 cells to doxorubicin (1.0 μM for 30 min) enhanced cellular respiration by 2−3-fold (Figure 1A,B and Table 1). This effect of the drug was completely prevented by caspase inhibition (Figure 3A,B), indicating that apoptotic signals were responsible for the enhancement. In contrast, in the resistant cells (HL-60/MX2, see Figure 5), the same treatment with doxorubicin was without effect on cellular respiration (Table 1, Figure 1C, and Figure 3C). Thus, the link between topoisomerase II and mitochondrial function appears to be

(39) Slee, E. A.; Zhu, H.; Chow, S. C.; MacFarlane, M.; Nicholson, D. W.; Cohen, G. M. Benzylooxycarbonyl-Val-Ala-Asp (Ome) fluormethylketone (Z-VAD.FMK) inhibits apoptosis by blocking the processing of CPP32. *Biochem. J.* **1996**, *315*, 21−24.

(40) Cantoni, O.; Sestili, P.; Cattabeni, F.; Grandi, M.; Giuliani, F. C. Cellular and molecular pharmacology of 4-epidoxorubicin in HeLa cells. *J. Cancer Res. Clin. Oncol.* **1989**, *115*, 373−378.

(41) Chang, B. K.; Gregory, J. A. Comparison of the cellular pharmacology of doxorubicin in resistant and sensitive models of pancreatic cancer. *Cancer Chemother. Pharmacol.* **1985**, *14*, 132−134.

(42) Bigioni, M.; Salvatore, C.; Bullo, A.; Bellarosa, D.; Iafrate, E.; Animati, F.; Capranico, G.; Goso, C.; Maggi, C. A.; Pratesi, G.; Zunino, F.; Manzini, S. A comparative study of cellular and molecular pharmacology of doxorubicin and MEN 10755, a disaccharide analogue. *Biochem. Pharmacol.* **2001**, *62*, 63−70.

(43) Zenebergh, A.; Baurain, R.; Trouet, A. Cellular pharmacology of detorubicin and doxorubicin in L1210 cells. *Eur. J. Cancer Clin. Oncol.* **1984**, *20*, 115−121.

(44) Vrignaud, P.; Londos-Gagliardi, D.; Robert, J. Cellular pharmacology of doxorubicin in sensitive and resistant rat glioblastoma cells in culture. *Oncology* **1986**, *43*, 60−66.

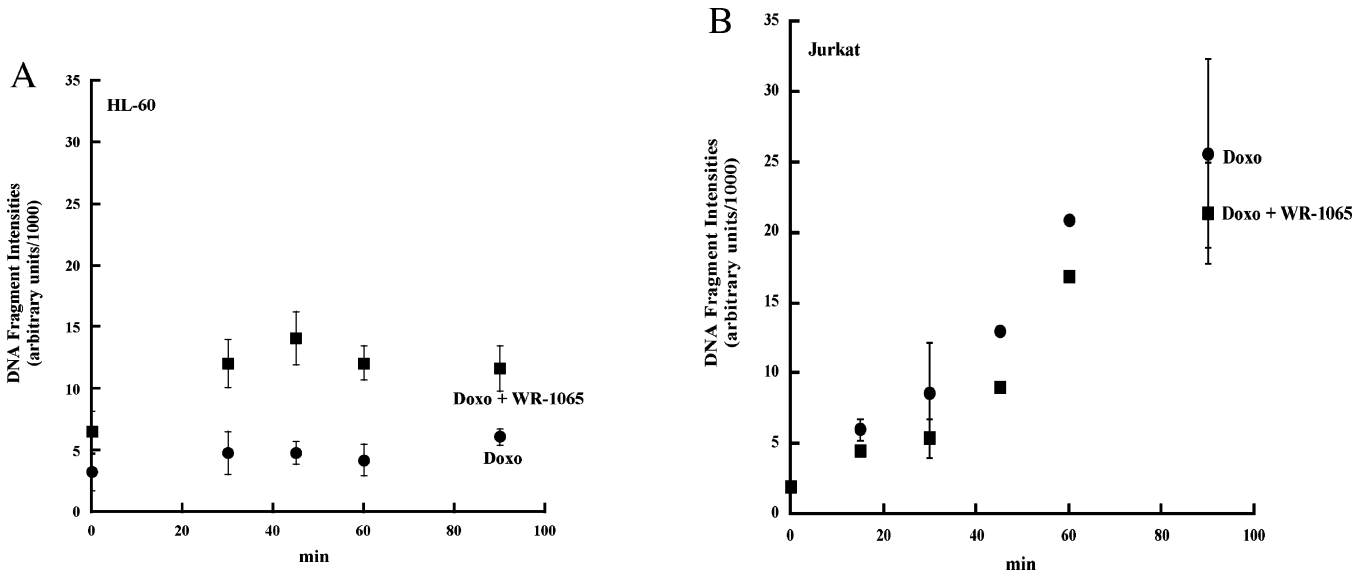

Figure 9. Doxorubicin-induced DNA fragmentation in the presence and absence of WR-1065. HL-60 (A) and Jurkat (B) cells were preincubated with (squares) and without (circles) 150 μM WR-1065 for 30 min. Doxorubicin (1.0 μM) was added and the incubations continued for the indicated periods of time. The cells were then maintained in medium with (squares) and without (circles) 150 μM WR-1065. The results are mean $\pm$ SD of 3 independent experiments for each cell line.

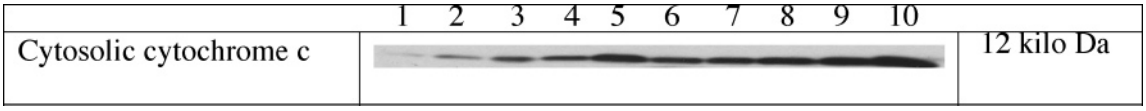

Figure 10. Doxorubicin-induced cytochrome *c* release. Jurkat (lanes 1−5) and HL-60 (lanes 6−10) cells were incubated with and without 1.0 μM doxorubicin for 15−90 min. Cytosolic extracts were prepared 24 h post doxorubicin exposure. Proteins (10 μg per condition) were separated by SDS−PAGE. Cytochrome *c* was probed and visualized as described in Materials and Methods. Lanes 1 and 6: Untreated cells. Lanes 2 and 7: Cells incubated with doxorubicin for 15 min. Lanes 3 and 8: Cells incubated with doxorubicin for 30 min. Lanes 4 and 9: Cells incubated with doxorubicin for 60 min. Lanes 5 and 10: Cells incubated with doxorubicin for 90 min.

due to inability to induce/execute apoptosis in response to doxorubicin in cells that are deficient in topoisomerase II.

It was reported that doxorubicin increased the permeability of the inner mitochondrial membrane by opening the mitochondrial PTP. In mammary adenocarcinoma cells, a high concentration of doxorubicin (17 μM for 60 min) decreased the value of $\Delta\Psi$m (measured 24 h after drug exposure) by about 30%, an effect that was blocked by zVAD-fmk.[8] Such an effect on $\Delta\Psi$m would be expected to uncouple phosphorylation from oxidation and to enhance respiration. In addition, doxorubicin increased the permeability of the outer mitochondrial membrane to cytochrome *c*[7] (Figure 10), an effect that might be expected to result in decreased mitochondrial respiration. However, we show here that cells exposed to doxorubicin exhibited an increased cellular mitochondrial oxygen consumption (Table 1) and cellular ATP content (Results), and that these increases occurred in spite of the leakage of cytochrome *c* (Figure 10, and other possible components) and the known opening of the mitochondrial PTP. The rate of cellular respiration was restored to normal in the presence of CSA, the inhibitor of the PTP (Figure 4A,B). Thus, it would appear that the PTP are responsible for or participate in doxorubicin-induced enhancement of cellular respiration. These results also show an active (accelerated) process of mitochondrial energy conversion in cells recovering from (or undergoing) doxorubicin-induced apoptosis. Among explanations for these observations are the possibility that cytochrome *c* leakage is partial (i.e., does not fully impair oxidations in the respiratory chain) or that newly synthesized cytochrome *c* replaces that which is lost. Moreover, the collapsed mitochondrial $\Delta\Psi$m (if it occurred under our conditions) might be transient and might not fully uncouple oxidative phosphorylation.[12] Cytochrome *c* is easily released in response to cell damage. However, even under a highly toxic cellular situation, the release does not fully deplete mitochondrial cytochrome *c* and a recovery in cellular respiration can be established by replacing cytochrome *c*.[45]

The mechanism responsible for the enhanced oxidative phosphorylation during recovery from apoptosis is unknown. A prolonged exposure to doxorubicin (1.0 μM for 2 h) inhibits mitochondrial oxygen consumption in Jurkat cells. Thus, it appears that the fate of cells exposed to toxins that

(45) Goldstein, J. C.; Munoz-Pinedo, C.; Ricci, J. E.; Adams, S. R.; Kelekar, A.; Schuler, M.; Tsien, R. Y.; Green, D. R. Cytochrome c is released in a single step during apoptosis. *Cell Death Differ.* **2005**, *12*, 453−462.

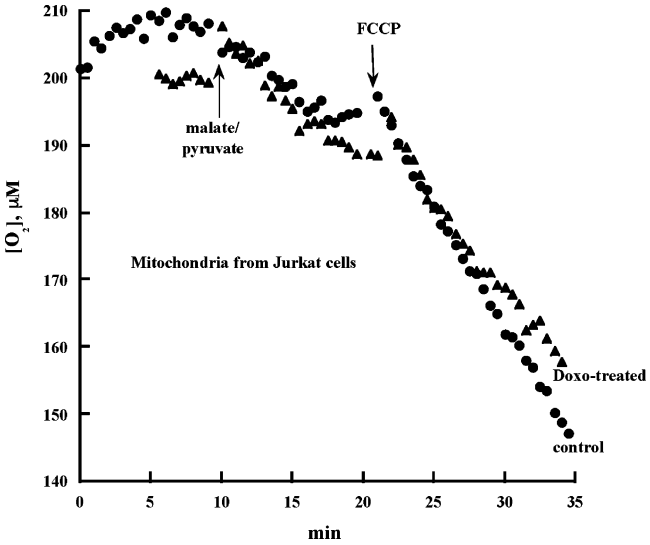

Figure 11. Oxygen consumption by isolated mitochondria from treated (triangles) and untreated (circles) cells. Jurkat cells were exposed to 1.0 μM doxorubicin for 30 min. At the end of the incubation period, the cells were washed and incubated in drug-free medium for 24 h. Mitochondria (0.4 mg per condition) were then isolated from the cells. Oxygen consumption was measured immediately as described in Materials and Methods. Where indicated, 10 mM respiratory substrate and 50 μM FCCP were added.

induce apoptotic signals could be recovery or death, depending on the magnitude of cellular insults. We show here that cells briefly exposed to doxorubicin show active oxidative phosphorylation. Whether or not stimulated respiration predicts cell recovery remains unknown. Similar stimulation of cellular respiration was observed with other cytotoxic agents, such as dexrazoxane and gossypol (data not shown).

Doroshow reported that high concentrations of doxorubicin (135 μM) stimulated oxygen consumption by isolated cardiac mitochondria. The stimulation was further enhanced by both KCN and rotenone. The overall increased oxygen consumption was attributed to the production of superoxide anion.[5] The enhancement of O_2 consumption was immediate, required NADH, and was stimulated by rotenone and cyanide. It was concluded that mitochondrial NADH dehydrogenase reduced doxorubicin to its semiquinone, with subsequent transfer of electrons to O_2.[5,6] For a variety of reasons, the stimulation of cellular mitochondrial oxygen consumption by doxorubicin under the conditions of the current study would appear to occur via a different mechanism (Table 1 and Figures 1−4). We used a low concentration (1.0 μM) and a brief exposure (30 min) to the drug. Although the final concentration of doxorubicin in our cells (calculated as cell doxorubicin content divided by cell volume) was roughly comparable to that used by Doroshow,[5] it does not follow that all of the doxorubicin associated with the cell would have access to the mitochondria. We also measured cellular respiration 24 h after drug exposure, rather than in the continuous presence of doxorubicin.[5] The observation that cell respiration was completely inhibited by rotenone and NaCN (Figure 2 and legend to Table 1) strongly supports the conclusion that the observed O_2 consumption occurred in the mitochondrial respiratory chain. Also, zVAD-fmk completely inhibited cellular respiration, suggesting that the enhanced O_2 consumption by doxorubicin treatment resulted from caspase activation. In addition, doxorubicin treatment increased the ATP content of the cells. It is unlikely that the mitochondria were permanently damaged by treatment of cells with doxorubicin since mitochondria isolated from treated and untreated cells showed similar sensitivity to the uncoupler FCCP (Figure 11).

Thus, it is clear that, in our experiments, doxorubicin treatment induces apoptosis, which increases mitochondrial oxidative phosphorylation (Tables 1 and 2 and Figures 1−4) in spite of drug-induced cytochrome *c* leakage (Figure 10) and possible opening of mitochondrial PTP. Moreover, in doxorubicin-treated cells, oxidative phosphorylation returned to normal in the presence of the mitochondrial PTP inhibitor CSA (Figure 4).

Topoisomerase II is the primary doxorubicin target.[2,3] Doxorubicin-induced DNA fragmentation is more pronounced in Jurkat cells (Figures 8 and 9), which has the highest topoisomerase II activity (Figure 6) and also accumulates more doxorubicin than HL-60 cells (Figure 7). zVAD-fmk decreased the fragment intensity by about 30% (Figure 8). This result is consistent with the earlier observation that doxorubicin-induced DNA breaks were not fully prevented by caspase inhibition.[8] The lower DNA fragmentation in HL-60 cells can be explained by the lower cellular doxorubicin accumulation (Figure 7C, squares) and topoisomerase II activity (Figure 6). DNA fragmentation in HL-60/MX2 cells is also low (data not shown), which is again thought to be due to the nature of topoisomerase II.[32]

Thus, the data show that oxidative phosphorylation is enhanced in cells briefly exposed to low concentrations of doxorubicin. This preserved mitochondrial function occurs despite the drug-induced leakage of cytochrome *c* and opening of mitochondrial PTP. Moreover, this biologic response to a brief toxic exposure is completely blocked by caspase inhibition, confirming that the enhancement is associated with induction of apoptosis. Clearly, these experiments should be distinguished from those with a continuous exposure to high concentrations of doxorubicin (e.g., 3−20 μM). Under these extreme conditions oxidative phosphorylation is inhibited within 2−3 h of drug exposure, and caspase inhibition produces a complete protection (manuscript submitted for publication).

The mechanism underlying the above-described enhanced respiration remains unknown. In this study, we investigated cells that were briefly exposed to doxorubicin and then incubated in drug-free media for 24 h. Our goal was to permit full biologic response to the toxic exposure. Under these conditions (and despite the leakage of cytochrome *c* and the opening of PTP), cellular oxygen consumption and ATP content were higher than those for the untreated cells. These findings may reflect altered metabolic regulation in an attempt to repair injuries in cells in which apoptosis is

induced but not fully executed. The increased metabolic activity is due to an increased ATP demand, rather than an uncoupling process.

NaCN markedly inhibited cellular oxygen consumption and ATP content. Thus, both processes were products of oxidations in the respiratory chain. Therefore, the results presented show that mitochondrial oxidative phosphorylation is not only preserved but also enhanced in cells exposed to doxorubicin under the conditions of our experiments.

Abbreviations

PTP, permeability transition pores; $\Delta\Psi$m, mitochondrial electrochemical (transmembrane) potential; Pd phosphor, palladium derivative of *meso*-tetra-(4-sulfonatophenyl)-tetrabenzoporphyrin; CSA, cyclosporin A; *k*, zero-order rate constant for cellular respiration; zVAD-fmk, benzyloxycarbonyl-Val-Ala-Asp-fluoromethylketone; kDNA, kinetoplast DNA.

MP050080J